

ADAPTIVE DETECTION IN COMPOUND-GAUSSIAN CLUTTER WITH INVERSE GAUSSIAN TEXTURE

Sijia Chen, Lingjiang Kong*, and Jianyu Yang

School of Electronic Engineering, University of Electronic Science and Technology of China, Chengdu, Sichuan 611731, China

Abstract—This paper mainly deals with the problem of target detection in the presence of Compound-Gaussian (CG) clutter with the Inverse Gaussian (IG) texture and the unknown Power Spectral Density (PSD). The traditional CG distributions, in particular the K distribution and the complex multivariate t distribution, are widely used for modeling the real clutter data from the High-Resolution (HR) radars. Recently, the novel CG distribution with the IG texture is described as the IG-CG distribution and validated to provide the better fit with the recorded data of the HR clutter than the mentioned two competitors. Within the IG-CG framework, the detector is firstly proposed here in terms of the two-step Generalized Likelihood Ratio Test (GLRT) criterion, and the empirical estimation method is resorted to estimate the unknown PSD in order to adapt the realistic scenario. The proposed detector is tested on the real-life HR clutter data, in comparison with the Adaptive Normalized Matched Filter (ANMF) processor, and the detection results illustrate that it outperforms the ANMF.

1. INTRODUCTION

Detection of a signal of interest in a background of clutter is a fundamental task in the radar systems [1]. Traditionally, the Gaussian distribution [2] is commonly utilized to model the low-resolution clutter. With the development of advanced technique, the High-Resolution (HR) radars [3–5] reduce the resolution cell size of the illuminated scenario, leading to that the statistical assumption of the Gaussian distribution for the HR clutter is not appropriate in the real world [6]. As a result, the conventional radar detectors, namely those

Received 12 December 2012, Accepted 11 January 2013, Scheduled 19 January 2013

* Corresponding author: Lingjiang Kong (lingjiang.kong@gmail.com).

designed to detect targets embedded in Gaussian disturbance, suffer the noticeable performance degradation under the condition of the HR clutter [7, 8].

Consequently, for the sake of accurately describing the distribution of the HR clutter to avoid the deterioration of the detection performance, the numerous research efforts are devoted to both the theoretical modeling of radar backscatter [9–11] and the statistical analysis of the recorded live data of the HR clutter [12–15]. These analyses show that as the range resolution increases, the clutter becomes correlated and heavy-tailed, and the model, the so-called Compound-Gaussian (CG) model, is suitable for clutter echoes from the HR radars and/or at the low grazing angles. The CG model is a physically motivated process, which can be mathematically described as Spherically Invariant Random Process (SIRP) of the produce of two components, speckle and texture, i.e., $\mathbf{c} = \sqrt{\tau}\mathbf{x}$ [16]. The speckle component \mathbf{x} represents the local backscattering, modeled as a circular, complex Gaussian vector, and the texture component τ , a nonnegative random variable, denotes the local clutter power fluctuation.

Within the CG class, the dissimilar selections of the texture model form the diverse CG distributions. The CG distribution with the Gamma texture, referred to as the classical K distribution [17] where the parameter estimation strategies of this distribution are introduced, presents a good fit with the real radar clutter data collected using the McMaster IPIX radar [18]. In [19], the corresponding detectors are derived in terms of the K distribution model, including the various Adaptive Normalized Matched Filters (ANMFs) with the discrepant estimation methods of the clutter covariance matrix. Additionally, the CG distribution with inverse Gamma texture, the so-called complex multivariate t distribution, is also proposed fit for the real measurements of the HR clutter [20, 21]. Meanwhile, the Maximum Likelihood (ML) and Method of Fractional Moments (MoFM) estimates are presented to find the parameters of the complex multivariate t distribution [20]. Subsequently, according to the model of the complex multivariate t distribution, the researchers propose the relevant detectors whose performance is close to that of the ANMF [22]. Recently, the novel CG distribution with the Inverse Gaussian (IG) texture, namely the IG-CG distribution, provides the better fit with the real-life HR clutter data than the widely used K distribution as well as the complex multivariate t distribution [23], where the ML is proposed for the parameter estimation of the IG-CG statistical distribution. However, to the best of the authors' knowledge, there is no detector based on the model of the IG-CG distribution in the literature.

As a consequence, we focus on the adaptive detection under the background of the IG-CG distribution clutter in this paper. Precisely, the detector is proposed in terms of the two-step Generalized Likelihood Ratio Test (GLRT) design procedure: first derive the GLRT for the assumption that the covariance matrix of the primary data (test data) is known, and then, the covariance matrix estimation by using the secondary data (training data) is substituted, in place of the true covariance matrix, into the test. Subsequently, the proposed adaptive detector and the existing ANMF processor are tested on the IPIX radar clutter data, and the performance of the proposed detector is superior to that of the ANMF.

The remainder of the paper is organized as follows. Firstly, in Section 2, the IG-CG model is described in detail. Secondly, the derivation of the proposed detector is given in Section 3. Thirdly, in Section 4, the performance analysis is presented, and finally, the conclusions are provided in Section 5.

2. SIGNAL MODEL

Assume that a radar transmits a coherent train of N Coherent Processing Interval (CPI) pulses in a single scan and that the receiver properly demodulates, filters, and samples the incoming waveform. The primary data vector $\mathbf{z} \in C^{N \times 1}$ (C being the complex field) is assumed to be sought in the resolution Cell Under Test (CUT), written as

$$\mathbf{z} = a\mathbf{p} + c \quad (1)$$

where a is the unknown and determinate parameter, and \mathbf{p} indicates the known steering vector. The secondary data $\mathbf{z}_k, k = 1, \dots, K$, are drawn from the adjacent range cells to the CUT, with the exclusion of a guard cell on either side of it to avoid target self-nulling.

As stated previously, the texture τ of the IG-CG model satisfies the inverse Gaussian distribution with shape parameter $\beta > 0$ and unit mean, whose Probability Density Function (PDF) is shown as [24]

$$\mathbf{p}_\tau(\tau) = \sqrt{\frac{\beta}{2\pi}} \tau^{-3/2} \exp\left(-\frac{\beta(\tau-1)^2}{2\tau}\right) \quad (2)$$

Additionally, the speckle component \mathbf{x} is a complex, circle, zero mean stationary Gaussian vector with the covariance matrix $\mathbf{M}_x = E[\mathbf{x}\mathbf{x}^H]$, where $(\cdot)^H$ denotes the complex conjugate transpose operation, and $E[\cdot]$ is the statistical expectation.

In the following, the detection problem to be solved can be

formulated in terms of the binary hypotheses test:

$$\begin{aligned} H_0: & \begin{cases} \mathbf{z} = \mathbf{c} \\ \mathbf{z}_k = \mathbf{c}_k, & k = 1, \dots, K \end{cases} \\ H_1: & \begin{cases} \mathbf{z} = a\mathbf{p} + \mathbf{c} \\ \mathbf{z}_k = \mathbf{c}_k, & k = 1, \dots, K \end{cases} \end{aligned} \quad (3)$$

According to the PDF of the IG-CG distribution in [23], the N -order PDF of \mathbf{z} under the condition of the hypothesis H_0 can be written as

$$\begin{aligned} & \mathbf{p}(\mathbf{z}|\mathbf{M}_x; H_0) \\ &= \frac{1}{\pi^N \|\mathbf{M}_x\|} h_N(q_0(\mathbf{z})) \\ &= \frac{1}{\pi^N \|\mathbf{M}_x\|} \int_0^\infty \tau^{-N} \exp\left(-\frac{q_0(\mathbf{z})}{\tau}\right) \mathbf{p}_\tau(\boldsymbol{\tau}) d\boldsymbol{\tau} \\ &= \frac{\sqrt{2\beta} \exp(\beta)}{\pi^{(N+\frac{1}{2})} \|\mathbf{M}_x\|} \cdot \left(1 + \frac{2q_0(\mathbf{z})}{\beta}\right)^{-\left(\frac{N}{2} + \frac{1}{4}\right)} \cdot K_{N+\frac{1}{2}}\left(\beta \sqrt{1 + \frac{2q_0(\mathbf{z})}{\beta}}\right) \end{aligned} \quad (4)$$

with

$$q_0(\mathbf{z}) = \mathbf{z}^H \mathbf{M}_x^{-1} \mathbf{z} \quad (5)$$

where $\|\cdot\|$ denotes the determinant of a square matrix, and $K_\varpi(\cdot)$ stands for the modified second-kind Bessel function of order ϖ .

Similarly, the PDF of \mathbf{z} under the condition of the hypothesis H_1 is shown as

$$\begin{aligned} & \mathbf{p}(\mathbf{z}|a, \mathbf{M}_x; H_1) \\ &= \frac{\sqrt{2\beta} \exp(\beta)}{\pi^{(N+\frac{1}{2})} \|\mathbf{M}_x\|} \cdot \left(1 + \frac{2q_1(\mathbf{z})}{\beta}\right)^{-\left(\frac{N}{2} + \frac{1}{4}\right)} \cdot K_{N+\frac{1}{2}}\left(\beta \sqrt{1 + \frac{2q_1(\mathbf{z})}{\beta}}\right) \end{aligned} \quad (6)$$

with

$$q_1(\mathbf{z}) = (\mathbf{z} - a\mathbf{p})^H \mathbf{M}_x^{-1} (\mathbf{z} - a\mathbf{p}) \quad (7)$$

3. IG-CG DETECTOR

The canonical GLRT detection strategy is given by

$$\Lambda_{\text{IG-CG}}(\mathbf{z}) = \frac{\max_{a, \mathbf{M}_x} \mathbf{p}(\mathbf{z}|a, \mathbf{M}_x; H_1)}{\max_{\mathbf{M}_x} \mathbf{p}(\mathbf{z}|\mathbf{M}_x; H_0)} \underset{H_0}{\overset{H_1}{\geq}} \gamma \quad (8)$$

where γ is the detection threshold to be set according to the desired value of the probability of false-alarm (P_{fa}).

Maximization in (8) is obtained by replacing the unknown parameters a and \mathbf{M}_x with their ML estimators. Unfortunately, joint maximization under the hypothesis H_1 is a rather difficult task, and to be the best of authors' knowledge, a closed-form solution does not exist.

Therefore, we resort to the two-step GLRT strategy. In the step one, the matrix \mathbf{M}_x is assumed to be known, and the two-step GLRT yields

$$\Lambda_{\text{IG-CG}}(\mathbf{z}) = \max_a \frac{\left(1 + \frac{2q_1(\mathbf{z})}{\beta}\right)^{-\left(\frac{N}{2} + \frac{1}{4}\right)} K_{N+\frac{1}{2}}\left(\beta\sqrt{1 + \frac{2q_1(\mathbf{z})}{\beta}}\right)}{\left(1 + \frac{2q_0(\mathbf{z})}{\beta}\right)^{-\left(\frac{N}{2} + \frac{1}{4}\right)} K_{N+\frac{1}{2}}\left(\beta\sqrt{1 + \frac{2q_0(\mathbf{z})}{\beta}}\right)} \underset{H_0}{\overset{H_1}{\geq}} \gamma \quad (9)$$

For the case at hand, the Maximum Likelihood Estimation (MLE) of a can be obtained as

$$\hat{a} = \frac{\mathbf{p}^H \mathbf{M}_x^{-1} \mathbf{z}}{\mathbf{p}^H \mathbf{M}_x^{-1} \mathbf{p}} \quad (10)$$

Substituting \hat{a} into (9), then, the test (9) reduces to

$$\Lambda_{\text{IG-CG}}(\mathbf{z}) = \frac{\left(1 + \frac{2\hat{q}_1(\mathbf{z})}{\beta}\right)^{-\left(\frac{N}{2} + \frac{1}{4}\right)} K_{N+\frac{1}{2}}\left(\beta\sqrt{1 + \frac{2\hat{q}_1(\mathbf{z})}{\beta}}\right)}{\left(1 + \frac{2q_0(\mathbf{z})}{\beta}\right)^{-\left(\frac{N}{2} + \frac{1}{4}\right)} K_{N+\frac{1}{2}}\left(\beta\sqrt{1 + \frac{2q_0(\mathbf{z})}{\beta}}\right)} \underset{H_0}{\geq} \gamma \quad (11)$$

with

$$\hat{q}_1(\mathbf{z}) = (\mathbf{z} - \hat{a}\mathbf{p})^H \mathbf{M}_x^{-1} (\mathbf{z} - \hat{a}\mathbf{p}) \quad (12)$$

Notice that the same symbol γ is used in (9) and (11) for the appropriate modifications of the original threshold in (8).

In the step two, for the purpose of adapting the IG-CG detector (11) to the unknown covariance matrix, the estimation of \mathbf{M}_x in the empirical analysis for the target detection is implemented by using [25]:

$$\hat{\mathbf{M}}_x = \frac{1}{K\hat{P}} \sum_{k=1}^K \mathbf{z}_k \mathbf{z}_k^H \quad (13)$$

in which \hat{P} is the estimated average clutter power of the training data:

$$\hat{P} = \frac{1}{KN} \sum_{k=1}^K \mathbf{z}_k^H \mathbf{z}_k \quad (14)$$

4. PERFORMANCE ASSESSMENT

For the purpose of the performance comparison, the existing ANMF is written as

$$\Lambda_{\text{ANMF}}(\mathbf{z}) = \frac{|\mathbf{p}^H \hat{\mathbf{M}}_x^{-1} \mathbf{z}|^2}{\left(\mathbf{p}^H \hat{\mathbf{M}}_x^{-1} \mathbf{p}\right) \left(\mathbf{z}^H \hat{\mathbf{M}}_x^{-1} \mathbf{z}\right)} \underset{H_0}{\overset{H_1}{\gtrless}} \gamma_{\text{ANMF}} \quad (15)$$

where $|\cdot|$ stands for the modulus of a complex number, and γ_{ANMF} is the detection threshold to be set according to the desired value of P_{fa} .

Precisely, the performance of both the Adaptive IG-CG (AIG-CG) detector and ANMF is evaluated in terms of P_{fa} and the probability of detection (P_d) with the measured clutter data from the McMaster IPIX radar. The radar site was located at east of the Place Polonaise at Grimsby, Ontario with location $43^\circ 12' 41''$ N, $79^\circ 35' 54'' 6$ W, looking at Lake Ontario from a height of 20 m. The carrier frequency of the radar is 9.39 GHz, and the Pulse Repetition Frequency (PRF) is 1 kHz where the polarizations HH and VV are available. The data have been preprocessed in order to get rid of the DC offsets of both I and Q channels and the phase imbalance due to hardware imperfections. As in [18], we focus the performance analysis on the data from the dataset files 19980223_165836_antstep, 19980223_170435_antstep, and 19980223_171533_antstep, taken at three different range resolutions, whose details are reported in Table 1.

The Signal-to-Clutter Ratio (SCR) is defined as

$$\text{SCR} = \frac{\sigma_a^2}{\sigma^2} \quad (16)$$

where σ_a^2 is the power of the target, and σ^2 is the average power of the real-life clutter data estimated from the corresponding file. Moreover, equivalent simulations against white Gaussian noise are utilized to set the nominal thresholds for the detectors since no theoretical expression relating the P_{fa} and threshold is available [26].

For illustration purpose, Figure 1 shows the detection curves of both AIG-CG detector and ANMF referred to the data of the three

Table 1. Data.

File	Cell	Range resolution (m)
19980223_165836_antstep	19th	30
19980223_170435_antstep	4th	15
19980223_171533_antstep	17th	3

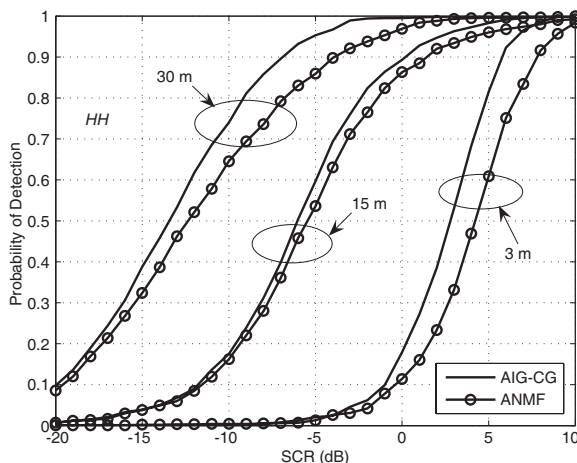


Figure 1. P_d versus SCR with the IPIX data, HH polarization, $N = 8$, $K = 24$, and $P_{fa} = 10^{-3}$.

Table 2. Kurtosis.

Resolution (m)	HH	VV
30	9.1127	5.1807
15	5.1807	6.8680
3	1.0698	-

files with HH polarization, where $N = 8$, $K = 24$, and $P_{fa} = 10^{-3}$. The results clearly manifest the performance advantage of the AIG-CG detector over the existing ANMF processor (approximately 1–3 dB better at $P_d = 0.9$). This can be explained by the fact that the derivation of the AIG-CG detector is based on the IG-CG statistical model which provides the superb fit for the considered data.

Additionally, the kurtosis κ is commonly the significant index of statistical distribution in the clutter modeling. In particular, the greater the value of kurtosis is, the spikier (or heavier-tailed) the distribution of the clutter data is, and naturally the smaller κ is, the distribution is closer to the complex Gaussian distribution. Precisely the values of κ for the considered data are reported in Table 2 as [23]. In Figure 1, it can be seen that the detection performance of the AIG-CG detector improves as the value of κ increases, inferring that the AIG-CG detector is appropriate for the heavier-tailed clutter with great potential.

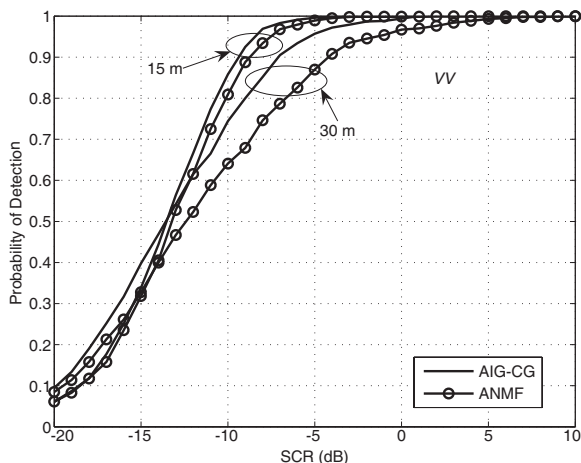


Figure 2. P_d versus SCR with the IPIX data, VV polarization, $N = 8$, $K = 24$, and $P_{fa} = 10^{-3}$.

For VV polarization, the empirical PDF is rejected for all the possible distributions for the data of the file 19980223_171533_antstep (3 m resolution) since the time course of the data in this file has a less continuous character compared with that in the other files [18, 23]. Hence, the value of κ for the data in the file 19980223_171533_antstep with VV polarization is not addressed, and Figure 2 reports the comparison results of the two detectors under the conditions of both 30 m and 15 m resolutions with VV polarization, where $N = 8$, $K = 24$, and $P_{fa} = 10^{-3}$.

As observed in Figure 2, the detection performance of the proposed AIG-CG processor is superior to that of ANMF (approximately 0.7–3 dB higher at $P_d = 0.9$). Considering that the value of κ for the data of 15 m resolution is a little higher than that of 30 m resolution, the performance of the AIG-CG detector under the former condition is slightly better than that under the latter one at most SCRs.

5. CONCLUSIONS

In this paper, the AIG-CG detector based on the CG model with the special IG texture is addressed and analyzed. More precisely, the AIG-CG detector is derived in terms of the two-step GLRT criterion and tested on the real data from the IPIX radar. The detection results show that the performance of the AIG-CG detector is better than that of the classical ANMF processor.

ACKNOWLEDGMENT

This work is sponsored by National Natural Science Foundation of China (Grant No. 61178068), Sichuan Youth Science and Technology Foundation (Grant No. 2011JQ0024), and the Fundamental Research Funds for the Central Universities (Grant No. ZYGX2012Z001). The authors are deeply in debt to Professor S. Haykin and Dr. B. Currie who have kindly provided the IPIX data in their website.

REFERENCES

1. Carretero-Moya, J., J. Gismero-Menoyo, A. Asensio-López, and Á. Blanco-del-Campo, "Application of the radon transform to detect small-targets in sea clutter," *IET Radar Sonar Navig.*, Vol. 3, No. 2, 155–166, 2009.
2. Kelly, E. J., "An adaptive detection algorithm," *IEEE Trans. Aerosp. Electron. Syst.*, Vol. 22, No. 1, 115–127, 1986.
3. Qu, Y., G. S. Liao, S. Q. Zhu, and X. Y. Liu, "Pattern synthesis of planar antenna array via convex optimization for airborne forward looking radar," *Progress In Electromagnetics Research*, Vol. 84, 1–10, 2008.
4. Qu, Y., G. S. Liao, S. Q. Zhu, X. Y. Liu, and H. Jiang, "Performance analysis of beamforming for MIMO radar," *Progress In Electromagnetics Research*, Vol. 84, 123–134, 2008.
5. Hatam, M., A. Sheikhi, and M. A. Masnadi-Shirazi, "Target detection in pulse-train MIMO radars applying ICA algorithms," *Progress In Electromagnetics Research*, Vol. 122, 413–435, 2012.
6. Carretero-Moya, J., J. Gismero-Menoyo, Á. Blanco-del-Campo, and A. Asensio-López, "Statistical analysis of a high-resolution sea-clutter database," *IEEE Trans. Geosci. Remote*, Vol. 48, No. 4, 2024–2037, 2010.
7. Watts, S., C. J. Baker, and K. D. Ward, "Maritime surveillance radar. II. Detection performance prediction in sea clutter," *IEE Proc.-F, Radar Signal Process.*, Vol. 137, No. 2, 63–72, 1990.
8. Conte, E., Lops, M., and Ricci, G., "Adaptive detection schemes in compound-Gaussian clutter," *IEEE Trans. Aerosp. Electron. Syst.*, Vol. 34, No. 4, 1058–1069, 1998.
9. Sangston, K. J. and K. R. Gerlach, "Coherent detection of radar targets in a non-Gaussian background," *IEEE Trans. Aerosp. Electron. Syst.*, Vol. 30, No. 2, 330–340, 1994.
10. Ward, K. D., R. J. A. Tough, and S. Watts, "Sea clutter: Scatter-

- ing, the K -distribution and radar performance,” *IET Radar Sonar Navig. Ser.*, Vol. 20, 45–95, 2006.
11. Haykin, S., R. Bakker, and B. W. Currie, “Uncovering nonlinear dynamics — The case study of sea clutter,” *Proc. IEEE*, Vol. 90, No. 2, 860–881, 2002.
 12. Greco, M., F. Bordonni, and F. Gini, “X-band sea-clutter nonstationarity: Influence of long waves,” *IEEE J. Oceanic Eng.*, Vol. 29, No. 2, 269–283, 2004.
 13. Greco, M., F. Gini, and M. Rangaswamy, “Non-stationarity analysis of real X-band clutter data at different resolutions,” *IEEE Radar Conf.*, 44–50, 2006.
 14. Ward, K. D., C. J. Baker, and S. Watts, “Maritime surveillance radar. I. Radar scattering from the ocean surface,” *IEE Proc. Radar Signal Process.*, Vol. 137, No. 2, 51–62, 1990.
 15. Nohara, T. J. and S. Haykin, “Canadian East Coast radar trials and the K -distribution,” *IEE Proc. Radar Signal Process.*, Vol. 138, No. 2, 80–88, 1991.
 16. Bandiera, F., O. Besson, and G. Ricci, “Knowledge-aided covariance matrix estimation and adaptive detection in compound-Gaussian noise,” *IEEE Trans. Signal Process.*, Vol. 58, No. 10, 5391–5396, 2010.
 17. Blacknell, D. and R. J. A. Tough, “Parameter estimation for the K -distribution based on $[z \log(\mathbf{z})]$,” *IEE Proc. Radar Sonar Navig.*, Vol. 148, No. 6, 309–312, 2001.
 18. Conte, E., A. De Maio, and C. Galdi, “Statistical analysis of real clutter at different range resolution,” *IEEE Trans. Aerosp. Electron. Syst.*, Vol. 40, No. 3, 903–918, 2004.
 19. Conte, E. and A. De Maio, “Mitigation techniques for non-Gaussian sea clutter,” *IEEE J. Oceanic Eng.*, Vol. 29, No. 2, 284–302, 2004.
 20. Balleri, A., A. Nehorai, and J. Wang, “Maximum likelihood estimation for compound-Gaussian clutter with inverse gamma texture,” *IEEE Trans. Aerosp. Electron. Syst.*, Vol. 43, No. 2, 775–779, 2007.
 21. Sangston, K. J., F. Gini, and M. S. Greco, “New results on coherent radar target detection in heavy-tailed compound-Gaussian clutter,” *IEEE Radar Conf.*, 779–784, 2010.
 22. Shang, X. and H. Song, “Radar detection based on compound-Gaussian model with inverse gamma texture,” *IET Radar Sonar Navig.*, Vol. 5, No. 3, 315–321, 2011.
 23. Ollila, E., D. E. Tyler, V. Koivunen, and H. V. Poor, “Compound-

- Gaussian clutter modeling with an inverse Gaussian texture distribution,” *IEEE Signal Process. Lett.*, Vol. 19, No. 12, 876–879, 2012.
24. Johnson, N. L., S. Kotz, and N. Balakrishnan, *Continuous Univariate Distributions*, Wiley-Interscience, New York, 1994.
 25. Carretero-Moya, J., J. Gismero-Menoyo, A. Asensio-López, and Á. Blanco-Del-Campo, “Small-target detection in high-resolution heterogeneous sea-clutter: an empirical analysis,” *IEEE Trans. Aerosp. Electron. Syst.*, Vol. 47, No. 3, 1880–1898, 2011.
 26. Pulsone, N. B. and R. S. Raghavan, “Analysis of an adaptive CFAR detector in non-Gaussian interference,” *IEEE Trans. Aerosp. Electron. Syst.*, Vol. 35, No. 3, 903–916, 1999.